Carpathian Journal of Earth and Environmental Sciences, August 2016, Vol. 11, No 2, p. 449 - 462

DETERIORATION OF GLAZED ARCHITECTURAL CERAMICS DUE TO ENVIRONMENTAL FACTORS: A COMPARATIVE STUDY OF TWO BUILDINGS IN BUDAPEST

Ágnes BARICZA[1], Bernadett BAJNÓCZI[2*], Máté SZABÓ[2], Mária TÓTH[2], Zsolt BENDŐ[3] & Csaba SZABÓ[1]

[1]Lithosphere Fluid Research Lab, Department of Petrology and Geochemistry, Institute of Geography & Earth Sciences, Eötvös Loránd University, H-1117 Budapest, Pázmány Péter sétány 1/C, Hungary, baricza.agnes@gmail.com, cszabo@elte.hu

*[2]Institute for Geological and Geochemical Research, Research Centre for Astronomy and Earth Sciences, Hungarian Academy of Sciences, H-1112 Budapest, Budaörsi u. 45, Hungary, bajnoczi.bernadett@csfk.mta.hu, *corresponding author toth.maria@csfk.mta.hu, szabo.mate@csfk.mta.hu,*

[3]Department of Petrology and Geochemistry, Institute of Geography & Earth Sciences, Eötvös Loránd University, H-1117 Budapest, Pázmány Péter sétány 1/C, Hungary, zsolt.bendo@gmail.com

Abstract: The Zsolnay products are one of the most famous Hungarian ceramics. The architectural ceramics produced by the Zsolnay Factory were often applied to decorate buildings, mainly around the turn of the 19th and 20th centuries. We have studied two buildings in Budapest, the Museum of Applied Arts in the densely built-up centre of the city with high traffic rate, and the Geological and Geophysical Institute of Hungary in a city quarter with moderate traffic and more open space. The main aim was to study the effects of the environmental factors (e.g. rainfall, gaseous pollutants in air, living forms) and the deterioration phenomena on the glazed roof tiles of the buildings. Two types of Zsolnay ceramics were examined: one from the building period and another one from the 20th century renovation periods of the buildings. The objects are similar in their ceramic bodies, but different regarding the covering glaze layers. Black deposition, traces of biological activity, and natural and artificial particles were identified on the ceramics of both buildings. A distinctive difference was the presence of gypsum frequently covering the objects of the Museum of Applied Arts. On some objects of this building pitting corrosion and weathering of the glaze were observed and lead was leached from the thin surface layer of the glaze as well as along cracks-microcracks in the glaze, in addition lead-rich depositions were precipitated. If weathering continues for a long period, it will result in the deterioration of the whole glaze.

Keywords: architectural ceramic, glaze, Zsolnay, deterioration, environmental factors, Budapest

1. INTRODUCTION

In the last decades much more attention is being paid to the influence of mankind on our environment than previously. All types of the building materials are continuously exposed to the environmental harmful factors (e.g. rainfall, gaseous pollutants in air, living forms) originating from physical, chemical or biological sources. Some decades ago the deterioration of building materials were slower, however, nowadays the rate of the deterioration is faster mainly in urban areas and densely populated cities (Grossi & Brimblecombe, 2007). In the 21st century one of the major roles of society is to conserve the historical and cultural heritage. These days it is well known how the environmental factors, like high traffic rate or gaseous pollutants, launch deterioration on natural building materials, e.g. carbonate rocks (limestone, marble), sandstones or volcanic rocks (e.g. Ausset et al., 1999; Török et al., 2011; Maravelaki-Kalaitzaki, 2005; Garcia-Vallés et al., 1998; McCabe et al., 2011; Monte, 2003).

It is widely accepted that "the high melting temperatures of ceramics and glasses implies that diffusion coefficients of most of the elements are too

low at ambient temperature to be significant at human lifespan and these materials are often considered to be corrosion resistant" (Tournié et al,, 2008). Contrarily, the air pollutants derived from different sources can damage ceramics and especially glasses easily if these silicate-based materials are exposed for a long time to the harmful factors (e.g. Schreiner, 2004; Gentaz et al., 2011; Robinet et al., 2007). However, there is not yet a comprehensive knowledge about the deterioration processes of the man-made artificial building materials, especially glazed architectural ceramics (for case studies see e.g. Pérez-Arantegui et al., 1997; Schwarz et al., 2003; Kopar & Ducman, 2007; Zhao et al., 2010; Donà, 2011; Madkour & Khallaf, 2012). The most common deterioration phenomena of a glaze are colour changing, soiling and crust formation, formation of microcracks, efflorescence and subflorescence of salts, exfoliation and flaking-off and surface corrosion (Schwarz et al., 2003).

The Zsolnay ceramic factory was established in Pécs (South Hungary) in 1853. At the top of its popularity, between 1875 and 1918, more than 150 buildings were covered with Zsolnay ceramics and applied by the most famous Hungarian architects (e.g. Ödön Lechner, Miklós Ybl and Alajos Hauszmann). The products of the factory were widely applied in the capital and other cities (e.g. Pécs, Szeged). Furthermore, they were also popularly used in the territory of historical Austro-Hungarian Empire (Pataky, 1962), especially because of their uniqueness and inimitable glaze colours.

The purpose of our study is to reveal the effects of environmental factors (e.g. rainfall, gaseous pollutants in air, living forms) on architectural ceramics (glazed roof tiles) produced by the Zsolnay factory and outplaced on two buildings (Museum of Applied Arts, Geological and Geophysical Institute of Hungary), which are located in different parts of Budapest. In order to determine the deterioration mechanisms and the present condition of the building ceramics, we have examined the degradation of the material, mostly the glaze, as well as the depositions accumulated on the tiles. The importance of our study is that the Zsolnay ceramics have not been studied in detail in this aspect before.

2. METHODS

The phase composition of the ceramic body and the depositions accumulated on the objects was determined by X-ray diffraction analysis (XRD) with a Philips PW 1730 diffractometer (analytical parameters: Cu Kα beam, 45 kV, 35 mA, 0.05°- 0.01° 2Θ step, 1 sec time constant, PW-1050/25 type goniometer, graphite monocromator, proportional counter detector) at the Institute for Geological and Geochemical Research in the Research Centre for Astronomy and Earth Sciences of the Hungarian Academy of Sciences (henceforth as RCAES HAS).

The surface of the glazed front and unglazed back sides of some selected ceramics was studied with an Amray 1830 I/T6 scanning electron microscope (SEM) with energy dispersive spectrometer (EDS) (analytical conditions: 20 kV accelerating potential, 1 nA beam current, focused electron beam, diameter: ~50 nm) at the Department of Petrology and Geochemistry of the Eötvös Loránd University and a FEI Quanta 3D dual beam scanning electron microscope (FIB-SEM) (analytical conditions: 20 kV accelerating potential, 4 nA beam current, focused electron beam, diameter: ~1 nm) at the Faculty of Science Research and Instrument Core Facility of the Eötvös Loránd University (ELTE FS-RICF). The SEM technique was also used to observe the microstructure of the ceramic body and the glaze, respectively, the ceramic-glaze interface and the alterations of the glaze, as well as the depositions on both sides of the objects on cross sections cut perpendicular to the ceramic-glaze interface.

The quantitative analysis of the unaltered and the deteriorated (weathered) glaze was done with a JEOL Superprobe-733 type electron microprobe equipped with an Oxford Instruments INCA Energy 200 energy dispersive spectrometer (EDS) (analytical conditions: 20 kv, 6 nA) at the Institute for Geological and Geochemical Research (RCAES HAS). Natural and artificial materials of the Taylor Co. (USA) and artificial glasses of the Smithsonian Institution (USA) were used as standards. PAP correction was automatically made by the Oxford Instruments software. The 'bulk' chemical composition of the intact glaze was determined by areal analyses with 300 s count time; the analysed areas were set as large as possible depending on glaze thickness and contained the typical inclusions such as quartz, feldspar and tin oxide. At least three area measurements were done on each glaze and the results were averaged. Several spot analyses with 50 s count time were performed for the determination of vitreous matrix composition and the results were also averaged. Weathered glaze, including pits on the surface and lead-rich accumulations inside the vitreous layer, as well as depositions on the weathered glaze were measured by spot analyses as well. The analytical totals of the latter measurements are sometimes as low as 64 wt. % mainly due to the possible presence of components that cannot be analysed and the irregular sample surface.

The black deposition layer on the objects was

studied by means of Raman microspectrometry. Raman measurements were done with a HORIBA Jobin–Yvon LabRAM HR edge filter-based, dispersive, confocal Raman microspectrometer (focal length 800 mm, 600 grooves/mm grating) at the Faculty of Science Research and Instrument Core Facility of the Eötvös Loránd University (ELTE FS-RICF). Point analyses were done using the 532 nm emission of a frequency-doubled Nd:YAG with a grating of 1800 grooves/mm. The maximum laser power incident on the sample was 40 mW.

3. MATERIALS AND ENVIRONMENT

3.1 The Zsolnay ceramics

The studied architectural ceramics were outplaced on two buildings in Budapest: the Museum of Applied Arts and the Geological and Geophysical Institute of Hungary. Both buildings were built in the 90s years of the 19th century (1893-96 and 1898-99, respectively) in Secession architectural style according to Ödön Lechner architect's plans (together with Gyula Pártos for the Museum of Applied Arts). The Museum is located in the densely built-up centre of Budapest with heavy traffic, whereas the Geological and Geophysical Institute is placed in a city quarter with moderate traffic and more open space (Fig. 1). During sampling we have collected ceramics of different ages (i.e. from the building and the 20th-century renovation periods) and with diverse glazes covered by a black deposition layer. Finally, 21 and 30 ceramic tiles, respectively, were collected from the two buildings (Fig. 1).

The studied ceramics of both buildings consist of two types of material. The first ceramic group composed of red body was outplaced in the building period, whereas the second ceramic group composed of white-yellow body was used in 1945-46 and after 1956, respectively (Fig. 1). Both ceramic bodies are composed of similar phases (quartz, cristobalite, mullite, K-feldspar, plagioclase and hematite) in different quantity indicating that bodies were made from kaolinite-bearing raw material (kaolin) and fired at 950-1200°C temperature (Baricza et al., 2015a).

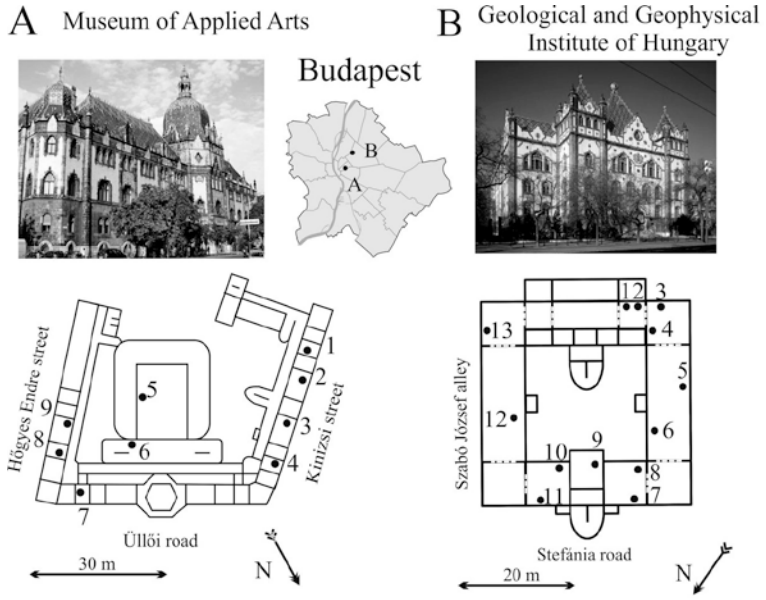

Sampling site	Sample name	Sample name
1	Institute/1-4	Museum/1-8
2	Institute/5-6	Museum/9-11
3	Institute/7-8	Museum/12
4	Institute/9-10	Museum/13-14
5	Institute/11	Museum/15
6	Institute/12-14	Museum/16-17
7	Institute/15	Museum/18
8	Institute/16-19	Museum/19-20
9	Institute/20-21	Museum/21
10	Institute/22-23	
11	Institute/24-26	
12	Institute/27-28	
13	Institute/29-30	

Age of ceramics	Samples
Museum of Applied Arts Group 1) building period, 1893-1896	Museum/6, 10, 12, 13B, 15, 19
Museum of Applied Arts Group 2) renovation period, after 1956	Museum/1, 2, 9, 11, 13A, 14, 16, 17
Geological and Geochemical Institute of Hungary Group 1) building period, 1898-1899	Institute/9, 10, 14, 16, 21, 23
Geological and Geochemical Institute of Hungary Group 2) renovation period, 1945-1946	Institute/1, 2, 4, 5, 6, 7, 8, 11, 12, 13, 17, 18, 19, 20, 22, 24, 25, 26, 27, 28, 29, 30

Figure 1. Location of the Museum of Applied Arts (A) and the Geological and Geophysical Institute of Hungary (B) on the schematic map of Budapest. On the schematic layout of the second floor of the buildings, the numbered dots indicate the sampling sites of ceramics. The table above shows the sampling sites and the belonging samples, the table below shows the representative samples of each group.

Table 1. Chemical composition of glazes of selected ceramics from the Museum of Applied Arts and the Geological and Geophysical Institute of Hungary (wt. %, areal and point analyses measured by using electron microprobe equipped by energy dispersive X-ray spectrometer, average ± standard deviation, n: number of measurements, thickness: average thickness of the glazes, n.a: not analysed, n.d: not detected).

Chemical composition (wt. %)	Museum of Applied Arts							
	First group				Second group			
	Museum/6 green		Museum/12 green		Museum/2 green		Museum/9 green	
	areal	point	areal	point	areal	point	areal	point
Na_2O	n.d.	n.d.	n.d.	n.d.	5.53 ± 0.26	5.41 ± 0.53	4.92 ± 0.21	4.85 ± 0.59
K_2O	1.00 ± 0.05	0.88 ± 0.11	0.68 ± 0.11	0.65 ± 0.18	1.19 ± 0.12	1.17 ± 0.11	1.25 ± 0.13	1.28 ± 0.31
CaO	1.35 ± 0.05	1.34 ± 0.19	1.12 ± 0.11	1.10 ± 0.21	5.16 ± 0.13	5.20 ± 0.25	4.66 ± 0.31	4.50 ± 0.82
MgO	0.39 ± 0.06	0.44 ± 0.17	n.d.	n.d.	0.23 ± 0.05	0.31 ± 0.11	0.23 ± 0.07	0.28 ± 0.11
ZnO	n.a.	n.a.	n.a.	n.a.	1.59 ± 0.25	1.53 ± 0.37	1.60 ± 0.34	1.23 ± 0.37
PbO	44.0 ± 0.8	46.5 ± 0.8	52.7 ± 0.4	51.9 ± 1.6	27.2 ± 0.5	27.7 ± 1.0	26.9 ± 0.6	26.7 ± 2.6
CuO	1.90 ± 0.13	2.01 ± 0.6	2.30 ± 0.10	2.18 ± 0.56	2.18 ± 0.16	2.14 ± 0.27	2.00 ± 0.04	2.00 ± 0.64
Al_2O_3	7.60 ± 0.44	7.29 ± 0.94	5.36 ± 0.42	5.51 ± 0.93	10.2 ± 0.5	9.80 ± 0.76	11.4 ± 0.3	11.2 ± 1.0
Fe_2O_3	0.72 ± 0.02	0.67 ± 0.14	0.64 ± 0.06	0.56 ± 0.49	1.10 ± 0.22	1.01 ± 0.22	1.13 ± 0.21	1.14 ± 0.19
SiO_2	39.7 ± 0.2	40.9 ± 1.8	37.2 ± 0.3	37.4 ± 1.6	38.2 ± 0.6	38.0 ± 0.8	38.0 ± 0.9	39.2 ± 3.2
TiO_2	0.39 ± 0.07	n.a.	n.a.	n.a.	n.a.	n.a.	n.a.	n.a.
Na_2O+K_2O+ CaO+MgO	2.74	2.66	1.8	1.75	12.11	12.09	11.06	10.91
Total	97.1 ± 0.8	100.0 ± 1.7	100.0 ± 0.3	99.3 ± 1.5	92.6 ± 0.7	92.3 ± 1.5	92.1 ± 0.9	92.4 ± 1.5
n	3	16	3	18	5	19	4	18
thickness (µm)	~ 200		~ 200		~ 270		~ 200	

Chemical composition (wt. %)	Geological and Geophysical Institution of Hungary							
	First group				Second group			
	Institute/9 light blue		Institute/10 dark blue		Institute/1 light blue		Institute/2 dark blue	
	areal	point	areal	point	areal	point	areal	point
Na_2O	1.64 ± 0.62	1.62 ± 0.44	1.19 ± 0.34	0.71 ± 0.28	6.43 ± 0.55	6.39 ± 0.50	7.51 ± 0.28	5.74 ± 1.64
K_2O	3.60 ± 0.32	4.38 ± 0.62	2.23 ± 0.13	2.29 ± 0.06	1.84 ± 0.05	2.01 ± 0.13	1.95 ± 0.24	2.16 ± 0.04
CaO	1.73 ± 0.52	1.44 ± 1.10	1.20 ± 0.08	1.30 ± 0.12	5.24 ± 0.54	6.82 ± 0.27	6.27 ± 0.29	6.79 ± 0.23
MgO	0.25 ± 0.11	0.32 ± 0.19	0.31 ± 0.23	n.d.	n.d.	n.d.	0.17 ± 0.30	n.d.
ZnO	0.98 ± 0.64	1.24 ± 0.67	3.22 ± 0.52	3.44 ± 0.35	1.50 ± 0.01	2.07 ± 0.29	2.73 ± 0.20	2.61 ± 0.22
PbO	14.7 ± 6.6	17.8 ± 5.4	28.5 ± 0.7	31.1 ± 0.5	12.8 ± 0.7	16.5 ± 1.1	15.3 ± 0.3	16.1 ± 0.5
CoO	n.d.	n.d.	0.77 ± 0.09	0.65 ± 0.14	n.d.	n.d.	0.48 ± 0.19	0.84 ± 0.38
Al_2O_3	11.6 ± 2.7	13.7 ± 5.3	9.86 ± 1.11	10.1 ± 0.4	12.4 ± 2.0	10.9 ± 0.8	10.8 ± 0.5	10.8 ± 0.3
Fe_2O_3	0.68 ± 0.28	0.57 ± 0.59	0.53 ± 0.17	0.48 ± 0.11	0.26 ± 0.24	0.82 ± 0.72	0.56 ± 0.13	0.99 ± 0.68
SiO_2	50.0 ± 5.4	53.1 ± 4.4	44.5 ± 1.0	47. 3 ± 1.0	50.0 ± 2.8	45.2 ± 1.0	40.3 ± 1.4	42.5 ± 0.9
SnO_2	9.1 ± 1.2	3.12 ± 3.26	5.29 ± 0.57	0.41 ± 0.36	3.82 ± 0.37	2.15 ± 0.65	6.68 ± 2.75	1.74 ± 0.21
Na_2O+K_2O+ CaO+MgO	7.22	7.76	4.93	4.3	13.51	15.22	15.9	14.69
Total	94.8 ± 3.0	97.9 ± 2.3	97.6 ± 03	97.8 ± 1.67	94.3 ± 1.2	92.9 ± 1.8	92.8 ± 1.0	90.3 ± 1.4
n	4	23	4	6	3	7	3	4
thickness (µm)	~ 210		~ 190		~ 210		~ 210	

The ceramics of the Museum of Applied Arts are covered by glazes with different chemical composition among the groups (Table 1). In the first group the ceramics were covered lead glazes (44-52 wt. % PbO, 37-41 wt. % SiO_2) with ~ 2-3 wt. % total alkali + alkaline earth ($Na_2O+ K_2O+CaO+MgO$) and ~5-7 wt. % alumina (Al_2O_3) content. In the second group the lead-bearing alkali glaze contains lower amount of lead oxide (~ 27 wt. % PbO, 38-39 wt. % SiO_2) and higher amount of total alkali + alkaline earth (~ 11-12 wt. % $Na_2O+ K_2O+CaO+MgO$) and alumina (~ 10-11 wt. % Al_2O_3) content. The glazes were coloured by copper (for green-coloured glaze) and iron (for yellow-coloured glaze) (Baricza et al., 2015a). However, the thickness of the glaze layers is similar among the groups between 200 and 270 µm.

The glaze layer on the ceramics of the Geological and Geophysical Institute show greater

variability in chemical composition (Table 1). The silica content of the glaze layer is between 40 and 53 wt. % SiO_2. The PbO content of the 'bulk' glaze is around 13-16 wt. % with the exception of one sample (Institute/10, first group) containing ~28 wt. % PbO. The total alkali + alkaline earth content (Na_2O+ K_2O+CaO+MgO) is ~4-8 wt. % in the glaze of the first group, whereas ~14-16 wt. % in the glaze of the second group. The alumina content is uniform (~10-12 wt. % Al_2O_3) among the glazes. The glazes contain tin oxide opacifier in 5-9 wt. % SnO_2 concentration in the glaze layer of the first group and in 4-7 wt. % SnO_2 concentration in the glaze layer of second ceramic group. The tin-opacified lead and lead-bearing alkali glazes of the Geological and Geophysical Institute are blue-coloured by cobalt dissolved in the vitreous matrix (Baricza et al., 2015a). The glaze thickness is around 200 μm.

The glaze of both ceramic groups is relatively homogeneous. The glaze of the first group of the Museum of Applied Arts ceramics contains a lot of needle-shaped, *in situ*-formed feldspar crystals in size of about 5-10 μm. The glaze of second ceramic group of this building contains some 50-100 μm sized, angular feldspar inclusions as relicts of the raw material. The glaze layer of both ceramic groups from Geological and Geophysical Institute contains lots of scattered and aggregated tin oxide crystallites as opacifier. The interface of the glaze layer and the ceramic body has different characteristics. In some tiles of the first ceramic group of both buildings the glaze soaked the upper part of the ceramic body resulting in a mixed layer (Baricza et al., 2015a). In the second group the glaze-ceramic body interface is sharp. The common feature of the glazes of both ceramic groups of the buildings is a reaction zone at the glaze-body interface due to diffusion of elements between the glaze and the ceramic body during firing (Baricza et al., 2015a). The reaction zone is composed of Pb-bearing K-Ca-Al-silicate phases.

3.2 Environmental conditions

The most important aspect in all types of degradation phenomena is the characteristics of the environment and the air quality of the locations of the buildings. According to the monitoring system of Hungarian Meteorological Institute (OMSZ), decreased levels of pollutants (SO_x, NO_x, CO, PM10 and PM2.5) were recorded in the past few years with the exception of PMs in Budapest (OMSZ 2013). However, the level of these pollutants can reach extremely high concentration in traffic peak times and during heating periods (Zichler et al., 2007). The concentration of the most problematic pollutant, the SO_2 decreased from an average of 63 μg/m^3 (1980) to 16 μg/m^3 (2004) and lately to 6 μg/m^3 (2008) (Zichler et al., 2007). Average concentrations of aerosol particles (including sulphate, nitrate, ammonium) decreased by 23% from 1980 to 2000 (66 μg/m^3/year) and further decreased to 35–40 μg/m^3 by 2008, due to a decrease in the background concentration. Nevertheless, recent data of monitoring stations of $PM_{2.5}$ and PM_{10} clearly reflect that fine dust exposure is still very high (compared to the previous pollutants in the city despite the decrease in the mean annual concentrations (OMSZ 2013).

4. RESULTS

The ceramics, depending on their exposure, are covered by a heterogeneous deposition layer (Fig. 2) made of (at least) two parts (X and Y on Fig. 2 G and H). The deposition layer contains Si, Al, P, Ca, K, Ba Fe, Mg and Pb and/or S, and the upper part (X on Fig. 2 G and H) contains higher amount of iron, phosphorus, lead and/or sulphur.

The deposition layer covers both the glazed front and the unglazed back sides of the ceramics, and occurs in great amount on the objects of the Museum. The thickness of the layer varies between 10 and 50 μm. The layer consists of dust, soot and fly ash in variable quantity. The deposition layer firmly adheres to the surface of the tiles, although rarely penetrates below the cracked glaze. The deposition often appears above cracks and fills the cracked glaze parts or holes (Fig. 2).

The XRD analysis indicates that the depositions on the ceramics of the Geological and Geophysical Institute contain variable amount of quartz, talc, chlorite, kaolinite, weddellite $Ca(C_2O_4)•2(H_2O)$ – whewellite $Ca(C_2O_4)•(H_2O)$, carbon-rich phase, hematite and other artificial iron phase (ferrite), as well as small amount of gypsum. The depositions on the Museum objects contain gypsum, weddellite, hematite (and FeOOH), thenardite and dolomite.

Lead sulphate $Pb(SO_4)_2(OH)_6$ was detected in the deposition of two ceramics (Museum/2 and 9, second ceramic group). Raman microspectrometry revealed presences of mica (mainly muscovite), hematite, chromium oxide and titanium-bearing particles in the deposition layer. On some ceramics (e.g. Institute/10 and 13, Museum/2 and 6) two other Raman peaks were observed: a characteristic broad peak of carbon-rich phase at 1590 cm^{-1} and another one at 1360 cm^{-1} (Fig. 3). Different types of spherules often appear on and in the deposition layer (Fig. 4). The size of the spherules varies between 5 and 50 μm in diameter.

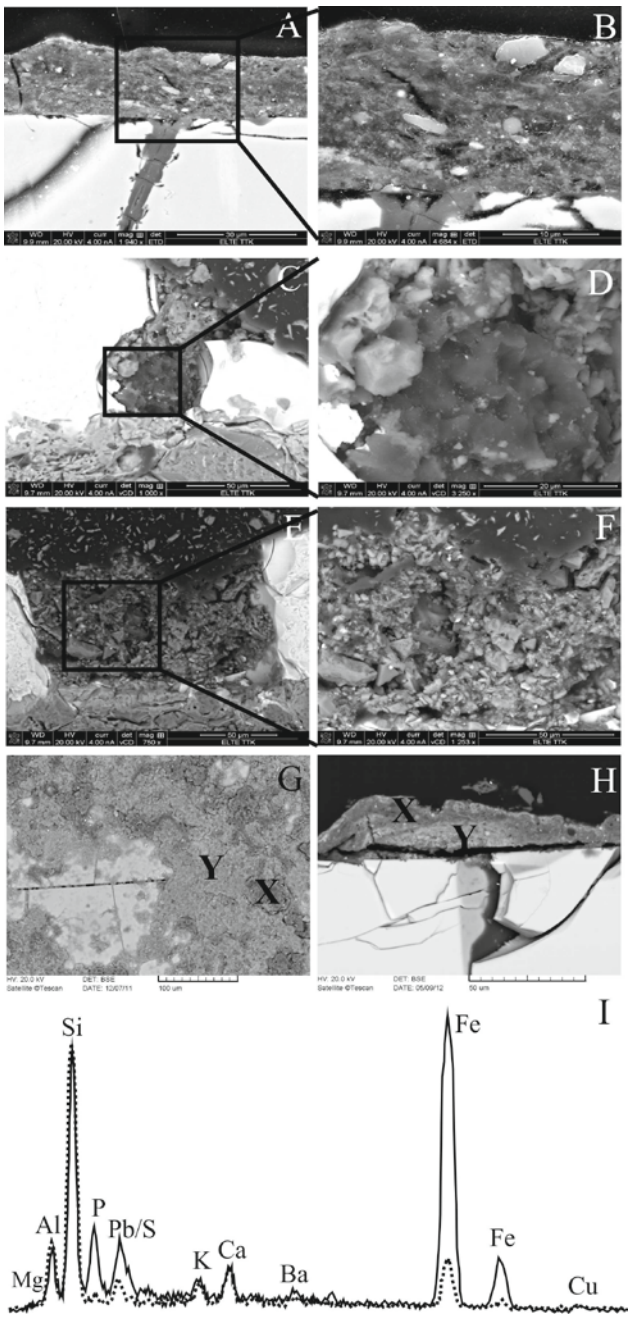

Figure 2. Deposition layer appears above cracks and fills the cracked glaze parts and holes (A-F) (Museum/1 and 2 samples, SE images) (Museum/2 and Institute/9 samples, BSE images). Plan-view (G) and side-view (H) images of the heterogeneous and layered deposition, which covers the glazed side of the ceramic (Museum/13a sample, BSE images). The energy-dispersive X-ray spectra (I) show the chemical composition of the deposition layers (X, upper part: straight line, Y, lower part: broken line).

The composition and morphology of the spherules is variable. By the SEM technique the carbonaceous spherules are dark and exhibit spongy morphology (Fig. 4 A), whereas other spherules (Fig. 4 B-D) are bright and occur in smooth and also in porous forms. The spherules appear both on the glazed front and the unglazed back sides of the ceramics, but preferentially anchor on the depositions on the glazed side.

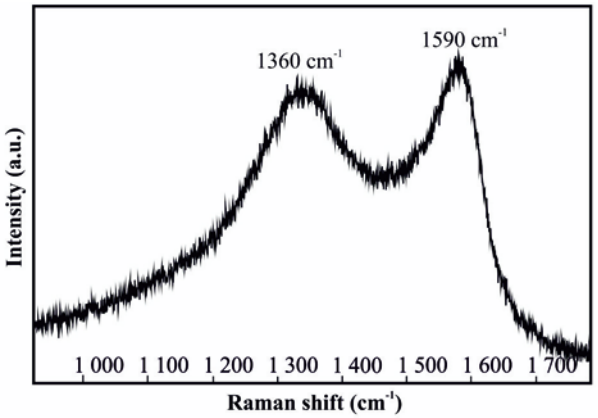

Figure 3. Raman spectrum from the deposition layer covering the surface of the ceramic (Museum/2 sample) showing a characteristic broad peak of carbon-rich phase ("disordered carbon"; Rosen & Novakov, 1977) at 1590 cm^{-1} and another one at 1360 cm^{-1}.

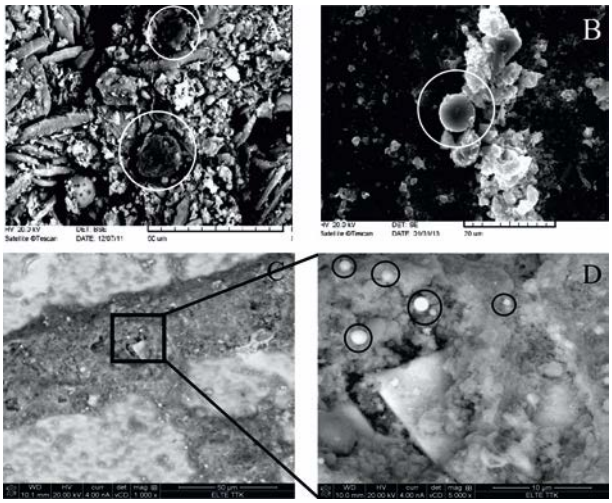

Figure 4. Spherules on the ceramics (indicated by circles). A) carbonaceous form (Museum/19 sample), B) Si-, Al-, K-, Ca-rich with small amount of Fe and Ti (Institute/9 sample), C-D) Fe-rich with small amount of Si (Museum/1 sample) (A, C, D - BSE images, B - SE images).

Among mineral salts gypsum, identified by SEM, accumulates mainly on the surface of the ceramic tiles of the Museum of Applied Arts. Gypsum is present in different forms (Fig. 5 A-D). On the back side of the tiles, dense, compact and laminar gypsum layer appears. Gypsum occurs in simple laminar and needle-like forms and in small amount on the glazed front side of the ceramics compared to the back side and it is often covered by the deposition layer. Furthermore, gypsum is present not only on the surface, but also in the cracks of the glaze (Fig. 5E).

In addition to gypsum, radial aggregates of

thenardite (Na_2SO_4) and glauberite ($Na_2Ca(SO_4)_2$) crystals (Fig. 5 F) are often present on the surface, especially in pits or cracks of the glaze of both buildings.

Both on the glazed and the unglazed sides of the ceramics traces of biological activity were found, which are probably residues of former microorganisms (bacteria, lichen and/or fungi). The most frequent residues are hyphae penetrating into the deposition layer or growing on the surface.

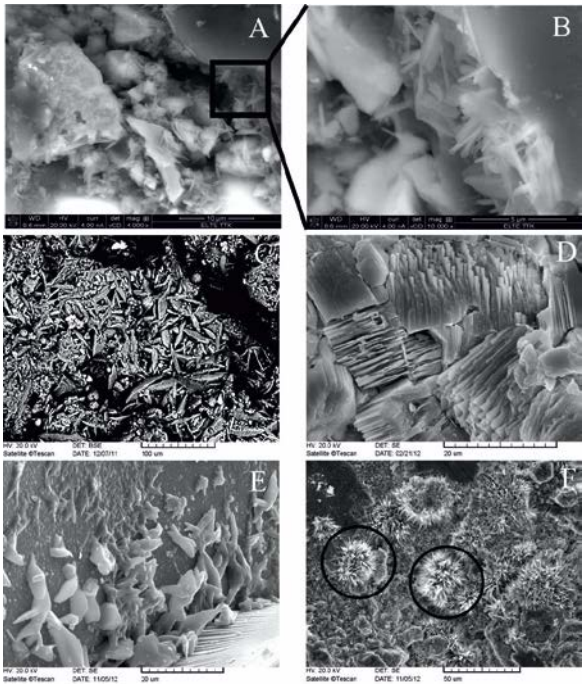

Figure 5. Gypsum and glauberite on the ceramics. A-B) needle-like gypsum appears in the deposition layer (Museum/1 sample, BSE image) C) dense, compact gypsum layer on the unglazed, back side of the ceramic (Museum/19 sample, BSE image), D) gypsum with laminar morphology on the unglazed, back side (Museum/6 sample, SE image), E) gypsum crystals in the cracks of the glaze (Museum/14, SE image), F) glauberite crystals on the ceramic body (Museum/15, SE image).

On the tiles of both buildings cracks and microcracks appear across the glaze, sometimes reaching the body-glaze interface and the ceramic body (Fig. 6). The greatest difference between the objects of the two buildings is that in the second ceramic group of the Museum lead-rich depositions are present in the cracks-microcracks of the glaze and at the body-glaze interface (Fig. 6, Table 2). Compared to the intact glaze layer of the Museum/9 sample (5.9-6.2 wt. % Na_2O, 1.2-1.7 wt. % K_2O, 4.0-4.8 wt. % CaO and 25.7-27.1 wt. % PbO), the deposition contains decreased amount of alkali and earth alkaline elements and increased amount of lead and phosphorous (0.5-3.2 wt. % Na_2O, 0.2-0.4 wt. % K_2O, 1.0-4.3 wt. % CaO, 22.4-50.6 wt. % PbO and 0.6-1.4 wt. % P_2O_5) (Table 2).

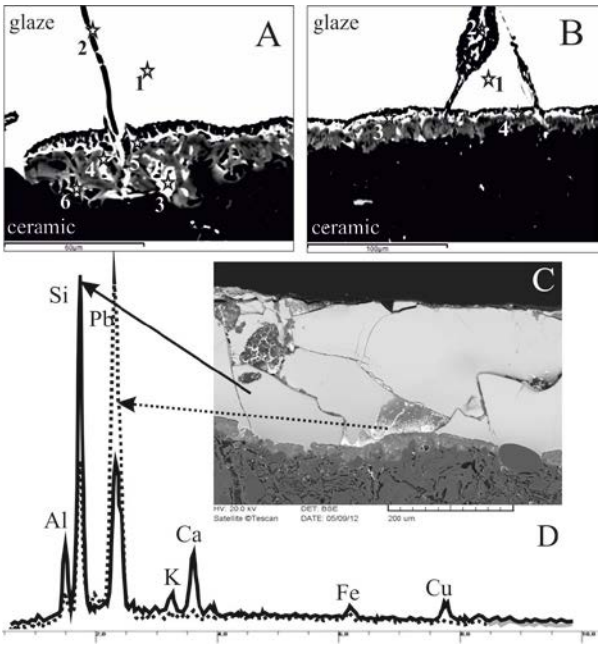

Figure 6. Degradation of the glaze. A-C) lead-rich depositions (white patches) in the microcracks and at the glaze-body interface where stars indicate the sites of the EDS measurements (Table 2) (Museum/9 sample, BSE images), D) Energy-dispersive X-ray spectra showing the chemical composition of the lead-rich accumulations in the glaze (dotted arrow) compared to chemical composition of the intact glaze (black arrow).

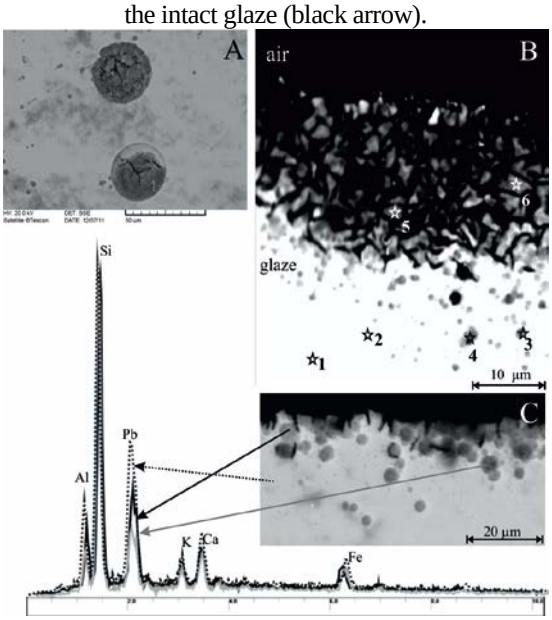

Figure 7. Pitting corrosion appears on the glaze surface and tends to the inner part. Cracks are formed at the edge of the pits. A) Plan view and B) side view of the pits and the cracks, stars indicate the sites of the EDS measurements (Table 3), C) side view of the pits with energy-dispersive X-ray spectra showing the chemical composition of a brighter pit (black arrow) and a darker pit (grey arrow) compared to that of the unaltered glaze (dotted arrow), (Museum/1 sample, BSE images).

Additionally, pits appear on the glaze surface of one ceramic from the Museum (Museum/1 sample) and cause the appearance of new cracks at their interface with the intact glaze (Fig. 7). The pits are in size of 2-10 μm with spherical shape. The pits show decreased amount of PbO, Na_2O, CaO and Al_2O_3 and increased SiO_2 content compared to the intact glaze (Table 3). A very thin (~5-10 μm) weathered layer appears on the glaze of some tiles from the Museum (second ceramic group, e.g. Museum/1, 2, 9) (Fig. 8). On top of the weathered glaze a deposition layer occurs. The deposition layer has higher amount of PbO than the weathered glaze, however, both the deposition and the weathered glaze have lower PbO content than the intact glaze. The microprobe analysis indicates that the weathered glaze can be highly depleted in lead, but its chemical composition can be varied based on the degree of degradation. In the Museum/2 sample, the weathered glaze in some points contains only 1.5 wt. % PbO compared to the 28 wt. % PbO content of the intact glaze, and the deposition layer contains ~4-5 wt. % PbO (Table 4 A, B). Similarly to the Museum/2 sample, in the Museum/9 sample the weathered glaze also has lower PbO content (6-17 wt. %) compared to the intact glaze (25-29 wt. % PbO), whereas the deposition layer on the top has 23 wt. % PbO content. However, deposition also occurs in the cracks of the glaze, in which increased PbO content (33 wt. % PbO) is observed (Table 4 C, D). The CaO, Na_2O, Al_2O_3 and CuO contents are lower in the deposition layer and in the weathered glaze parts than in the intact (unweathered) glaze. High amount of iron and phosphorus (up to 20 wt. % of Fe_2O_3 and 5 wt. % of P_2O_5) occurs only in the deposition layer (Fig. 8, Table 4).

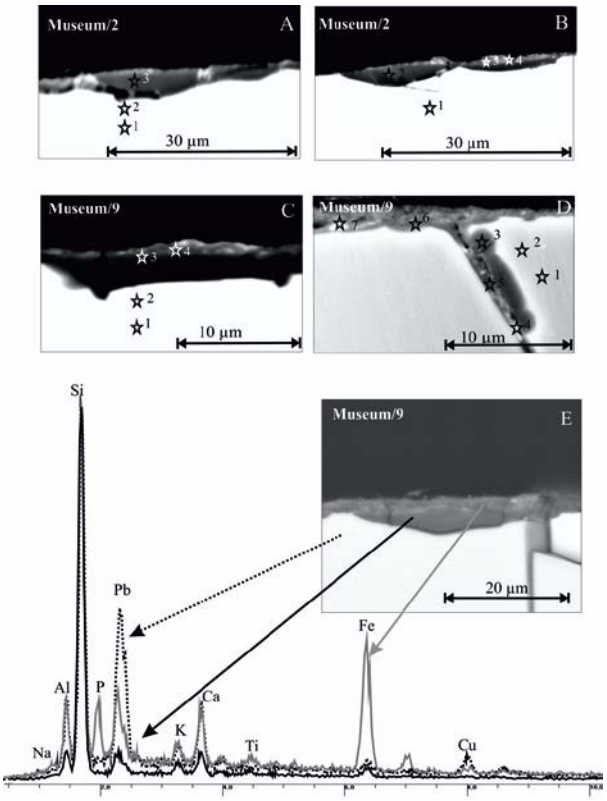

Figure 8. A-E) Cross-section of two glazed ceramic tiles (Museum/2 and Museum/9) showing the upper light grey deposition layer, the dark grey weathered glaze and the unaltered glaze beneath. Energy dispersive X-ray spectra show the chemical composition of the deposition layer (grey line), the weathered glaze (black line) and the unaltered glaze (dotted line). The numbered stars show the sites of the EDS measurements (Table 4). (A-C: BSE images, D-E: SE images).

Table 2. Chemical composition of the glaze and the depositions in the microcracks and at the body-glaze interface. Fig. 6 A and B show the sites of the point analyses (Museum/9) (wt. %, point analyses, n.d: not detected).

A) Museum/9 sample	Type of the glaze part	Na_2O	MgO	Al_2O_3	SiO_2	P_2O_5	SO_3	K_2O	CaO	Fe_2O_3	CuO	BaO	PbO	Total
1	glaze	6.16	0.28	11.5	37.5	n.d.	n.d.	1.15	4.82	1.31	2.02	n.d.	27.1	91.2
2	deposition	0.61	n.d.	3.25	20.5	0.98	5.54	0.19	1.61	2.47	n.d.	n.d.	22.4	57.5
3	deposition	0.39	n.d.	4.52	13.3	0.79	13.2	0.44	0.93	0.38	n.d.	n.d.	50.6	84.6
4	deposition	3.23	n.d.	14.0	37.2	0.85	7.77	0.29	2.64	0.36	n.d.	n.d.	34.0	100.2
5	deposition	0.49	n.d.	6.68	27.9	1.10	11.1	0.22	0.99	0.40	n.d.	6.83	27.0	82.8
6	deposition	0.86	n.d.	12.6	23.3	1.07	6.47	0.29	4.29	0.71	n.d.	n.d.	23.2	72.8

B) Museum/9 sample	Type of the glaze part	Na_2O	MgO	Al_2O_3	SiO_2	P_2O_5	SO_3	K_2O	CaO	TiO_2	Fe_2O_3	CuO	ZnO	PbO	Total
1	glaze	5.92	0.31	13.4	40.4	0.08	n.d.	1.65	3.97	0.22	1.19	1.46	1.44	25.7	94.8
2	deposition	n.d.	0.27	1.58	4.00	1.04	13.6	n.d.	n.d.	0.62	0.13	n.d.	n.d.	42.7	64.0
3	deposition	1.23	n.d.	12.0	11.6	0.62	10.2	0.21	1.54	0.98	0.65	n.d.	n.d.	36.4	75.4
4	deposition	1.31	0.18	6.24	15.0	1.39	10.4	0.23	0.99	1.67	1.57	n.d.	n.d.	38.1	77.0

Table 3. Chemical composition of the intact glaze (points 1-2) and the pits (points 3-6) (Museum/1 sample) (wt. %, n.d: not detected). Fig. 7 B shows the sites of the point analyses.

Measured points	Na_2O	MgO	Al_2O_3	SiO_2	K_2O	CaO	TiO_2	Fe_2O_3	ZnO	PbO	Total
1 - glaze	2.80	n.d.	9.03	32.6	1.66	4.39	0.36	3.00	1.22	25.7	80.7
2 - glaze	2.58	n.d.	8.99	33.7	1.43	4.04	0.39	3.22	1.17	25.7	81.2
3 - pit	2.09	n.d.	8.93	38.2	1.33	4.16	n.d.	2.60	1.52	23.3	82.1
4 - pit	2.29	n.d.	8.01	30.6	1.42	4.24	n.d.	3.27	1.29	23.1	74.2
5 - pit	0.66	n.d.	6.61	42.6	1.24	3.05	n.d.	3.17	1.18	16.5	75.0
6 - pit	1.21	n.d.	7.97	45.7	1.43	3.41	0.31	2.90	0.93	19.1	82.9

Table 4. Chemical composition of the unaltered and the weathered glaze and the deposition layer (Museum/2, Museum/9) (wt. %, point analyses, n.d: not detected). Fig. 8 A-D shows the sites of the point analyses.

A) Museum/2 sample	Type of the glaze part	Na_2O	MgO	Al_2O_3	SiO_2	P_2O_5	SO_3	K_2O	CaO	TiO_2	Fe_2O_3	CuO	ZnO	PbO	Total
1	glaze	5.44	0.36	9.82	38.1	n.d.	n.d.	1.20	5.37	n.d.	0.59	2.64	1.37	27.7	92.7
2	glaze	3.99	n.d.	8.75	43.1	n.d.	n.d.	1.17	4.93	n.d.	1.58	2.60	1.51	24.9	92.5
3	weathered glaze	n.d.	n.d.	5.85	70.3	1.26	1.94	0.81	0.86	n.d.	1.14	n.d.	n.d.	1.49	83.6

B) Museum/2 sample	Type of the glaze part	Na_2O	MgO	Al_2O_3	SiO_2	P_2O_5	SO_3	K_2O	CaO	TiO_2	Fe_2O_3	CuO	ZnO	PbO	Total
1	glaze	4.89	0.39	9.15	39.1	n.d.	n.d.	1.21	5.54	n.d.	0.53	3.27	1.76	27.8	93.6
2	weathered glaze	0.81	0.72	5.17	68.6	0.41	2.79	0.84	2.58	n.d.	1.07	n.d.	n.d.	1.77	84.8
3	deposition	0.96	0.28	5.73	64.7	0.52	2.36	0.84	2.45	0.38	1.83	0.56	n.d.	4.85	85.4
4	deposition	1.07	1.07	5.73	34.7	2.32	3.46	0.71	2.19	0.68	7.64	n.d.	n.d.	4.51	64.0

C) Museum/9 sample	Type of the glaze part	Na_2O	MgO	Al_2O_3	SiO_2	P_2O_5	SO_3	K_2O	CaO	TiO_2	Fe_2O_3	CuO	ZnO	PbO	Total
1	glaze	5.09	0.47	11.5	37.6	n.d.	n.d.	1.14	4.74	n.d.	1.18	3.09	1.33	28.7	94.9
2	glaze	4.02	0.00	11.3	47.5	n.d.	n.d.	1.22	4.97	n.d.	1.26	3.82	1.41	27.1	102.6
3	weathered glaze	1.09	0.32	6.28	69.4	n.d.	4.16	1.11	3.37	0.41	1.33	0.56	n.d.	6.44	94.5
4	deposition	0.61	2.46	5.79	27.6	5.36	2.54	0.48	2.13	0.60	19.8	n.d.	n.d.	5.28	72.6

D) Museum/9 sample	Type of the glaze part	Na_2O	MgO	Al_2O_3	SiO_2	P_2O_5	SO_3	K_2O	CaO	TiO_2	Fe_2O_3	CuO	ZnO	PbO	Total
1	glaze	3.77	0.31	10.7	39.2	n.d.	n.d.	1.19	4.57	n.d.	1.40	4.28	1.26	27.2	93.9
2	glaze	2.32	0.33	10.1	40.7	n.d.	n.d.	1.00	4.18	n.d.	0.88	3.94	1.65	25.7	90.8
3	weathered glaze	1.18	n.d.	9.08	48.8	n.d.	n.d.	1.08	3.50	0.34	1.77	2.95	n.d.	17.1	85.8
4	deposition	1.45	n.d.	7.39	38.4	0.91	6.18	1.09	2.35	n.d.	1.20	1.41	1.08	33.0	94.5
5	weathered glaze	0.92	n.d.	6.94	56.6	n.d.	2.70	1.46	1.67	0.33	1.28	0.63	n.d.	11.3	83.9
6	deposition	0.44	0.53	8.50	43.7	4.23	3.20	0.53	3.18	0.50	6.41	1.00	0.78	11.4	84.4
7	deposition	1.79	n.d.	8.41	44.0	0.92	3.58	0.85	3.77	0.61	1.80	2.26	n.d.	23.0	91.0

5. DISCUSSION

In generally, the deterioration mechanisms are controlled by two main processes: 1) deposition layer forming on the surface of the objects and 2) leaching, cracking and other corrosion processes on the surface as well as inside of the objects (e.g. Ionescu et al., 2012).

5.1 Formation of deposition layer

A distinct deposition layer with variable amounts of spherules, minerals and salts accumulated on the surface of the ceramics of both buildings (Figs. 2, 4, 5), however, thicker deposition layer (up to 40 μm, Fig. 2H) is more often observed on the tiles from the Museum of Applied Arts. There are some general criteria for the appearance of such layer based on the experiments of Rodriguez-Navarro & Sebastian (1996) on calcareous stones in Granada, Spain. The first step is to accumulate dust and aerosol from natural and artificial sources on the glazed surface of the roof tiles with the help of the rainfall and other precipitations. The second step is the sulphation process from the gaseous pollutants, like sulphur dioxide, which easily starts forming gypsum from the accumulated Ca-bearing particles in wet conditions. If these criteria are passed, the layer will thicken due to the deposition of new aerosols, dusts and salts (Hutchinson et al., 1992; Rodriguez-Navarro & Sebastian, 1996; Ausset et al, 1999) and also exert a physically pressure that destroys the fabric of ceramic or the glaze layer beside the chemical degradation (Grossi & Brimblecombe, 2007).

The composition of the deposition layer was found to be related to the concentration of SO_2 and the total suspended particles in the air (Sabbioni, 2003). Since the Museum is located in the densely built-up centre of Budapest with high traffic rate and closed place, it is exposed to the emitted artificial and natural particles to a greater extent than the Institute which is located rather in an open place (Fig. 1). The mineralogical composition of the deposition layer (e.g. quartz, feldspar, dolomite, mica, chlorite, kaolinite) on the studied ceramics reflects mostly the surrounding geological environment as Márton et al., (2012) concluded based on their study on settled dust at Budapest. Beside the minerals of geological origin, oxalate phases (whewellite-weddellite), carbon-rich phase, hematite and gypsum were identified on the tiles from Geological and Geophysical Institute and in addition thenardite, lead sulphate and higher amount of gypsum were observed on the tiles from the Museum of Applied Arts.

The frequent appearance of gypsum, found in great amount (Fig. 5) especially on the ceramics of the Museum, can originate from several sources. The most probable is that gypsum and/or Ca-rich dust settles down from the atmosphere to the surface of the ceramic and (re)crystallizes as gypsum. Sipos et al., (2014) observed that the most frequent particle in the collected settled dust is gypsum in Budapest, although on the glazed side a small amount of gypsum might have been originated from the weathering of the glaze (see below). On the back side of the ceramics the source of gypsum can be the gypsum-bearing binder (mortar) used to fix the tiles and/or it can also form by the reaction of sulphur dioxide and carbonate.

Whewellite and weddellite are often referred to be minerals of biological origin (Verrecchia et al., 1993; Monte, 2003; Lluveras et al., 2008). Hyphae found on the surface of the ceramics also support the existence of present-day and/or former biological activity (Rampazzi et al, 2004). The oxalate phases could have been generated by the reaction of a calcium-bearing phase and oxalic acid produced by bacteria/fungi/lichen (Schiavon, 2002). Such organic minerals could also originate from biomineralization of microorganisms (Del Monte et al, 1987).

Thenardite observed on the ceramics mainly originates from natural sources. Some researchers have stated that this salt could be precipitated through seepage evaporation (Figueiredo et al., 2007), but others identified this phase in the deposition or patina layer of silicate-based materials, as glass or glaze, together with oxalate minerals and gypsum (Aulinas et al., 2009). Additionally, Steiger et al., (2011) determined that more than 70 evaporite minerals, together with thenardite, can be precipitated in the temperature range of -40 to +40ºC on the buildings. The building materials usually contain the most common ions (i.e. Na^+, K^+, Mg^{2+}, Ca^{2+}), which are needed for the precipitation of evaporates. Because thenardite mainly occurs on the ceramics from the Museum, which building has more deteriorated condition than the Institute, thus the needed ion (Na^+) is easily available via the degraded glaze layer, the in situ formation of thenardite is highly probable. However, it should be noted that evaporates, like thenardite, are not necessarily found where they were formed, except for the case of gypsum. Based on its relatively low solubility, gypsum tends to accumulates in the "black deposition layer", which develops in rain-protected areas. The remaining salts are far more soluble (one or two orders of magnitude higher than that of gypsum), thus they are usually completely dissolved if the pore space of the material is filled with precipitation (Steiger et al., 2011).

The observed carbon-rich phase (Fig. 3), hematite and lead sulphate phases in the deposition layer are also found in the environment. However, they are preferentially originated from artificial sources or made by human activities (e.g. from domestic heating, transport and industry) (Lefévre & Ausset 2002). Lead sulphate could originate from the lead-bearing glaze via ion exchange between the glaze and the contacting precipitation (see later) (Mohamed et al., 1995; Rahimi et al., 2009).

Other artificial particles found on the surface of

the ceramic tiles are the spherules (Fig. 4). Similar spherules were observed in the attic and settled dusts collected from the studied buildings (Baricza et al., 2015b). There are three main types of the identified artificial spherules: porous carbonaceous particles, metal particles mainly composed of iron and smooth aluminosilicate particles, which classification is confirmed by the literature as well (e.g. Del Monte et al., 1981; Sabbioni & Zappia, 1992; Sabbioni, 1995; Tanosaki et al., 2009). The source and influence of these particles are different according to their physical and chemical characteristics. The importance of carbonaceous particles (Fig. 4 A) is double: (i) they are responsible for the blackening of the deposition layer, and they can support the sulphation processes via their high sulphur content (Ausset et al., 1999), (ii) and they can become nucleation cores since their spongy-like texture is suitable for catching other particles (Bonazza et al., 2005). The iron-rich particles (Fig. 4 D) have catalytic effects on ambient SO_2 molecules, based on that Fe, with other elements like Ni, V or Cr, is able to accelerate the SO_2 oxidation into sulphate with the use of other elements such as Ca or Na (Sabbioni, 1995), which also occur in the glaze layer (Table 1). Therefore, it is not a surprise that gypsum crystallites appear on the glaze surface of the ceramics from the Museum of Applied Arts (Fig. 5). The aluminosilicate spherules also can contain iron, thus can catalyse the sulphation process (Sabbioni, 1995) mentioned above. Moreover, these particles also contain calcium, which can locally form gypsum crystals.

The characteristic Raman peaks of the deposition layer at 1590 cm^{-1} and 1360 cm^{-1} are attributed to “disordered carbon” as a secondary product of diesel or gasoline combustion (Rosen & Novakov, 1977) (Fig. 3). Moreover, Sadezky et al., (2005) also identified broad Raman peaks at around 1350 cm^{-1} and 1585 cm^{-1} in industrial soot particles. These data confirm that the observed carbon-rich phase originates from artificial sources, especially from the traffic via burning processes of the vehicles, mainly from diesel-engines, based on that more than 70 % of their emission consists of carbon particulate matter (soot or carbonaceous particles) (Rodriguez-Navarro & Sebastian, 1996).

The high amount of iron and phosphorus identified in the deposition layer of the ceramics from the Museum (Figs. 2 and 8, Table 2 and 4) is mainly attributed to artificial influences in the case of iron, and natural influences in the case of phosphorus, respectively. Iron is the most abundant metal at all (Sabbioni & Zappia, 1992; Torfs & Vangrieken, 1997), which mainly originates from the abrasion of vehicles or degradation of any other metal-rich equipment in urban area. The phosphorus is primarily related to the excrement of the local fauna, especially birds. From these elements, only the iron can increase the extent of the degradation of the glaze layer via its catalytic effect in SO_2 oxidation process (see above) on the surface of the material (Ausset et al., 1999).

5.2 Deterioration of glaze

Leaching, cracking and corrosion phenomena were identified on the glazes of the ceramics from the Museum (Figs. 6-8). These phenomenon could be originated from (i) gaseous pollutants emitted by traffic or industry (e.g. the SO_x and CO_2 gases, ammonia), which are able to form acids (e.g. sulphurous-sulphuric acids or weaker carbonic acid) with the surrounding precipitation (Chambers, 1976) and launch the sulphation process (see above) by starting to form gypsum or other sulphate minerals (thenardite, glauberite) (Fig. 5) observed on the glaze layer of the ceramics from the Museum, or (ii) living forms (biodeterioration), identified on some tiles from the Museum which can make undesired change (e.g. active penetration and leaching) in the material properties due to the activity of microorganisms or organisms belonging to various systematic groups. The corroded samples (mainly Museum/1, 2, 9) contain more evidences of the harmful effect of sulphation due to the presence gaseous pollutants than the biodeterioration (i.e. presence of sulphate minerals and thick deposition layer with gypsum and spherules).

The first step in the development of the deterioration phenomena of the glaze is the appearance of precipitation (e.g. rain, air humidity) and depending on the type of the contacting precipitation and its pH value dissolving, leaching, surface corrosion or relict products can occur (White, 1992). The weathering of the glaze on some tiles (Museum/1, 2, 9), or similar vitreous material like glass, starts with the leaching of alkali and alkali earth metals from the surface resulting in a weak layer on the top of the material (Fig. 8, Table 4). The leached (de-alkalinised) layer, often called “gel layer”, starts forming and it is often described as a silica-rich, hydrated material (Leisner, 2003; Tournié et al., 2008). Beside the leaching process, we have also observed cracks-microcracks and the pitting corrosion phenomenon - mainly on the glaze of the second group of the Museum ceramics (Fig 7, Table 3), these deterioration phenomena develop in the material because the glaze continuously depletes in its ingredients (Schreiner, 2004). We have identified these complex deterioration phenomena on some ceramics of the second group of the Museum (Figs. 6-

8, Table 2-4). The reason for the occurrence of these deterioration phenomena can be the unfavourable environment (more polluted city centre) compared to the Institute, which circumstances can launch the premature degradation of the ceramic tiles. This process is confirmed by differences in the conditions of the ceramics from the buildings studied. Most of the evidences of the corrosion were observed on the glaze of the Museum ceramics (i.e. greater amount of cracks-microcracks, pitting corrosion, weathering and leaching of the glaze, greater amount of deposition layer with sulphate minerals and artificial spherules). However, the greater total alkali and alkaline earth content in the glaze of the second ceramic group of the Museum compared to the first ceramic group can also induce weathering because these elements (e.g. Na, K) (Table 1) are less resistance in acidic environment ("acidic" rain) (Woisetschlager et al., 2000).

The observed weathered glaze layer is equal to the depleted "gel-layer" (Tournié et al., 2008). The elements (Ca, Na, Pb, Cu) leached from the weathered glaze have migrated to the upper deposition layer, which consists of additional particles from the atmosphere. The uppermost deposition layer contains gypsum (in greater amount on the ceramics of the Museum), which can partly originate from the reaction between the Ca content of the weathered glaze and the sulphuric acid. Moreover, this deposition layer contains thenardite and lead sulphate as well. The latter phases could also be developed through the reactions by the leached elements and the sulphuric acid (Ionescu et al., 2012). The lead leached from the weathered glaze has not totally migrated to the uppermost deposition/accumulation layer; it also accumulates along the cracks and microcracks of the glaze.

6. CONCLUSION

The results of the present work indicate what influences cause the premature ageing of the built environment if it is made of a special man-made material, the glazed ceramic, and emphasize the importance of the location of the building which can increase the extent of deterioration, especially in the urban environment.

Our purpose was to assess and compare the deterioration condition of Zsolnay architectural ceramics covering two buildings (the Museum of Applied Arts, in the densely built-up centre of the city and the Geological and Geophysical Institute of Hungary) in Budapest. The architectural ceramics studied are partly from the building period and partly from the 20th-century renovation periods of the buildings; the objects are similar in their ceramic bodies, but different regarding the covering glaze layers. Direct relationship between the deterioration status of the ceramics and their location on the buildings was not found. However, it is clearly seen that the ceramics of the second group (20th-century renovation period) of the Museum of Applied Arts are more degraded compared to the first ceramic group (building period).

We have identified similarities in the deterioration among the architectural ceramics of both buildings, such as deposition layer on the tiles, natural particles and artificial spherules in the deposition layer and traces of biological activity. The most conspicuous difference is the appearance of gypsum in great amount on the ceramics of the Museum of Applied Arts, which can indicate that this building is in better circumstances for gypsum mineralization (enough ingredients, time and place) and the sulphation process is in progress. In addition, we have demonstrated that in some tiles of the Museum of Applied Arts the glaze has already started to corrode (weather) on the surface and along cracks-microcracks reaching the body-glaze interface. If this phenomenon continues for a long period, it will result in the deterioration of the whole glaze. The ceramics of the Museum of Applied Arts are in worse condition, perhaps due to the location of the building.

Acknowledgement

Dr. Imre Takács (Museum of Applied Arts) and Dr. Tamás Fancsik (Geological and Geophysical Institute) are greatly acknowledged for their kind permission to carry out this study. The authors thank Gabriella Balla, Kornélia Hajtó and Katalin Csontos their help and contribution during the sampling. We are also grateful to Réka Káldos, Dániel Leányfalvi, Alexandra Müller, Olga Komoróczy, Zoltán Dankházi and Gábor Varga for their help in sampling, preparation and analysis.

This is publication No. 78 of the Lithosphere Fluid Research Lab at Eötvös Loránd University, Budapest in cooperation with the Institute for Geological and Geochemical Research, Research Centre for Astronomy and Earth Sciences, Hungarian Academy of Sciences.

REFERENCES

Aulinas, M., **Garcia-Valles, M.**, **Gimeno, D.**, **Fernandez-Turiel, J. L.**, **Ruggieri, F.** & **Puhés, M.,** 2009, *Weathering patinas on the medieval (S. XIV.) stained glass windows of the Pedralbes Monastery*, Environmental Science and Pollution Research, 16, 443-452.

Ausset, P., **Del Monte, M.** & **Lefévre, R.A.,** 1999, *Embryonic sulphated black crusts on carbonate rocks in atmospheric simulation chamber and in the field: role of carbonaceous fly ash*, Atmospheric

Environment, 33, 1525-1534.

Baricza, Á., Bajnóczi, B., Szabó, M., Szabó, Cs. & Tóth, M., 2015a, *Comparative material examination of Zsolnay architectural ceramics of different age*, Archeometriai Műhely (Archeometry Workshop), XII, 1, 33-50. (in Hungarian)

Baricza, Á., **Bajnóczi, B.**, **Tóth, M.**, **Káldos, R.** & **Szabó, Cs.**, 2015b, *Characterisation of particulate matter in attic and settled dusts collected from two buildings in Budapest, Hungary*, In: Sustainable Use of Traditional Geomaterials in Construction Practice, Geological Society, London, Special Publications, 416. doi: 10.1144/SP416.14

Bonazza, A., **Sabbioni, C.** & **Ghedini, N.,** 2005, *Quantitative data on carbon fractions in interpretation of black crusts and soiling on European built heritage*, Atmospheric Environment, 39, 2607-2618.

Chambers, L. A., 1976, *Classification and extent of air pollution problems*, In: Stern, A. C. (Ed.), Air Pollution, Third edition, Volume I., Academic Press, New York, 3-22.

Del Monte, M., **Sabbioni C.** & **Vittori O.,** 1981, *Airborne carbon particles and marble deterioration*, Atmospheric Environment, 15, 645-652.

Del Monte, M., **Sabbioni, C.** & **Zappia, G.,** 1987, *The origin of calcium oxalates on historical buildings, monuments and natural outcrops*. Science of the Total Environment, 67, 17-39.

Donà, V., 2011, *Diagnostica e monitoraggio del degrado di manufatti ceramici di valore storico - artistico: la facciata dell'Hotel Hungaria a Venezia Lido*. PhD thesis, Università degli Studi di Padova, 179 p.

Figueiredo, C. A. M., **Aires-Barros, L.**, **Basto, M. J.**, **Graca, R. C.** & **Maurício, A.,** 2007, *The weathering and weatherability of Basílica da Estrela stones, Lisbon, Portugal*, In: Přikryl, P. & Smith, B. J. (Eds.), Building Stone Decay: from diagnosis to conservation, Geological Society, London, Special Publication, 271, 99-107.

Garcia-Vallés, M., **Vendrell-Saz, M.**, **Molera, J.** & **Blazquez, F.,** 1998, Interaction of rock and atmosphere: patinas on Mediterranean monuments, Environmental Geology, 33, 1-2, 137-149.

Gentaz, L., **Lombardo, T.**, **Loisel, C.**, **Chabas, A.** & **Vallotto, M.,** 2011, *Early stage of weathering of medieval-like potash-lime model glass: evaluation of key factors*, Environmental Science and Pollution Research, 18, 291-300.

Grossi, C. M. & **Brimblecombe, P.,** 2007, *Effect of long-term changes in air pollution and climate on the decay and blackening of European stone buildings*, In: Přikryl, P. & Smith, B. J. (Eds.), Building Stone Decay: from diagnosis to conservation, Geological Society, London, Special Publications, 271, 117-130.

Hutchinson, A. J., **Johnson, J. B.**, **Thompson, G. E.**, **Wood, G. C.**, **Sage P. W.** & **Cooke M. J.,** 1992, *The role of fly-ash particulate material and oxide catalysis in stone degradation*. Atmospheric Environment 26A, 15, 2795-2803.

Ionescu, A., **Lefévre, R. A.**, **Brimblecombe, P.** & **Grossi, C. M.,** 2012, *Long-term damage to glass in Paris in a changing environment*, Science of the Total Environment, 431, 151-156.

Kopar, T. & **Ducman, V.,** 2007, *Low-vacuum SEM analysis of ceramic tiles with emphasis on glaze defects characterisation*, Materials Characterisation, 58, 1133-1137.

Lefévre, R. A. & Ausset, P., 2002, *Atmospheric pollution and building materials: stone and glass*. In: Siegesmund, S., Weiss, T. & Vollbrecht, A. (Eds): Natural stone, weathering phenomena, conservation strategies and case studies, Geological Society, London, Special Publications 205, pp. 329-345.

Leisner, J., 2003, *The effects of air pollution on glass*. In: Brimblecombe, P. (Ed.): The effects of air pollution on the building environment. Air pollution Reviews, Vol. 2, Imperial College Press, 249-263.

Lluveras, A., **Boularand, S.**, **Roqué, J., Cotte, M.**, **Giráldez, P.** & **Vendrell-Saz, M.,** 2008, *Weathering of gilding decorations investigated by SR: development and distribution of calcium oxalates in the case of Sant Benet de Bages (Barcelona, Spain)*, Applied Physics A, 90, 23-33.

Madkour, F. S. & **Khallaf, M. K.,** 2012, *Degradation process of Egyptian faience tiles in the step pyramide at Saqqara*, Procedia – Social and Behaviour Sciences, 68, 63-76.

Maravelaki-Kalaitzaki, P., 2005, *Black crusts and patinas on Pentelic marble from the Parthenon Erechteum (Acropolis, Athens): characterisation and origin*, Analitica Chimica Acta, 532, 187-198.

Márton, E., **Zajzon, N.**, **Lautner, P.**, **Sipos, P.**, **Szentmarjay, T.** & **Pethe, M.,** 2012, *Magnetic monitoring, geochemical and mineralogical analysis of settled dust from North and Central Transdanubia, Hungary*, Central European Geology, 55, 4, 347-364.

Mohamed, N., **Chin, Y. M.** & **Pok, F. W.,** 1995, *Leaching of lead from local ceramic tableware*, Food Chemistry, 54, 245-249.

Monte, M., 2003, *Oxalate film formation on marble specimens caused by fungus*, Journal of Cultural Heritage, 4, 255-258.

McCabe, S., **Smith, B.**, **Adamson, C.**, **Mullan, D.** & **McAllister, D.,** (2011, *The "Greening" of natural stone buildings: quartz sandstone performance as a secondary indicator of climate change in the British Isles*, Atmospheric and Climate Sciences, 1, 165-171.

OMSZ 2013, *Summary report of the air quality in Hungary. Annual report of the Hungarian Meteorological Institute (OMSZ) for the year 2012*, 111 p. (in Hungarian)

Pataky, D., 1962, *A Zsolnay kerámia. Múzeumi füzetek*, Janus Pannonius Múzeum, Pécs, 59 p.

Pérez-Arantegui, J., **Lapuente, P.**, **Punter, P.** & **Castillo, J. R.,** 1997, *Characterisation and alterations of Hispano-moresque tiles of 14th century*, Key

Engineering Materials, 132-136, 1493-1495.

Rahimi, R. A., **Sadrnezhaad, S. K.**, **Raisali, G.**, **Hamidi**, **A.,** 2009, *Hydrolysis kinetics of lead silicate glass in acid solution*, Journal of Nuclear Materials, 389, 427-431.

Rampazzi, L., **Andreotti, A.**, **Bonaduce, I.**, **Colombini, M. P.**, **Colombo, C.** & **Toniolo, L.,** 2004, *Analytical investigation of calcium oxalate films on marble monuments*, Talanta, 63, 967-977.

Robinet, L., **Eremin, K.**, **Coupry, C.**, **Hall, C.** & **Lacome N.,** 2007, *Effect of organic acid vapors on the alteration of soda silicate glass*, Journal of Non-Crystalline Solids, 353, 1546-1559.

Rodriguez-Navarro, C. & **Sebastian, E.,** 1996, *Role of particulate matter from vehicle exhaust on porous building stones (limestone) sulfation*, The Science of the Total Environment, 187, 79-91.

Rosen, H. & **Novakov, T.,** 1977, *Raman scattering and the characterization of atmospheric aerosol particles*. Nature, 266, 708-710.

Sabbioni, C., 1995, *Contribution of atmospheric deposition to the formation of damage layers*, The Science of the Total Environment, 167, 49-55.

Sabbioni, C., 2003, *Mechanisms of air pollution damage to stone*, In: Brimblecombe, P. (Ed.): The effects of air pollution on the built environment, Chapter 3, Air Pollution Reviews – Vol 2., Imperial College Press, 62-106.

Sabbioni, C. & **Zappia, G.,** 1992, *Atmospheric-derived element tracers on damaged stone*, The Science of the Total Environment, 126, 35-48.

Sadezky, A., **Muckenhuber, H.**, **Grothe, H.**, **Niessner, R** & **Pöschl, U.,** 2005, *Raman microspectroscopy of soot and related carbonaceous materials: Spectral analysis and structural information.* Carbon, 43, 1731-1742.

Schiavon, N., 2002, *Biodeterioration of calcareous and granitic building stones in urban environments*, In: Siegesmund, S., Weiss, T. & Vollbrecht, A. (Eds): Natural stone, weathering phenomena, conservation strateges and case studies, Geological Society, London, Special Publications, 205, 195-205.

Schreiner, M., 2004, *Corrosion of historic glass and enamels*, In: Janssen, K. & Van Grieken, R. (Eds.): Non-destructive microanalysis of cultural heritage materials. Comprehensive Analytical Chemistry XLII, Elsevier, 713-754.

Schwarz, H-J., **Freyburg, S.**, **Mottner, P.** & **Stadlbauer, E.,** 2003, *Conservation and restoration of glazed architectural ceramics in northern Germany*, In: Alva Balderrama, A., Almagro Vidal, A. & Bestué Cardiel, B. (eds.): El estudio y la conservación de la cerámica decorada en arquitectura, ICCROM Conservation Studies 1, Roma, 38-41.

Sipos, P., **Márton, E.**, **May, Z.**, **Németh, T.** & **Kovács, K. V.,** 2014, *Geochemical, mineralogical and magnetic characteristics of vertical dust deposition in urban environment*, Environmental Earth Science, 72, 905-914.

Steiger, M., **Charola, A. E.** & **Sterflinger, K.,** 2011 *Weathering and deterioration*, In: Siegesmund S. & Snethlage, R. (eds.): Stone in architecture, Springer Berlin Heidelberg, 227-316.

Tanosaki, T., **Watanabe, Y.**, **Ishikawa, Y.**, **Nambu, M.**, **Lin, J.**, **Yu, Q.** & **Nagataki, S.,** 2009, *Characterisation of east Asian fly ash by polarization microscope*, World of coal ash (WOCA) conference – May 4-7, 2009 in Lexington, KY, USA. http://www.flyash.info

Torfs, K. & **Vangrieken, R.,** 1997, *Chemical relations between atmospheric aerosols, deposition and stone decay layers on historic buildings at the Mediterranean coast*, Atmospheric Environment, 31, 15, 2179-2192.

Tournié, A., **Ricciardi, P.** & **Colomban, P.,** 2008, *Glass corrosion mechanism: A multiscale analysis*, Solid State Ionics, 179, 2142-2154.

Török, Á., **Licha, T.**, **Simon, K.** & **Siegesmund, S.,** 2011, *Urban and rural limestone weathering: the contribution of dust to black crust formation*, Environmental Earth Sciences, 63, 675-693.

Verrecchia, P. E., **Dumont, J-L.** & **Verrecchia, K. E.,** 1993, *Role of calcium oxalate biomineralization by fungi in the formation of calcretes: a case study from Nazareth, Israel*, Journal of Sedimentary Petrology, 63, 5, 1000-1006.

White, W. B., 1992, *Theory of corrosion of glass and ceramics.* In: Clark, D. E. & Zoitos, B. K. (eds.): Corrosion of Glass, Ceramics and Ceramic Superconductors. Principles, testing, characterization and applications. Noyes Publications, 1-27.

Woisetschlager, G., **Dutz, M.**, **Paul, S.** & **Schreiner, M.,** 2000, *Weathering phenomena on naturally weathered potash-lime-silica-glass with medieval composition studied by secondary electron microscopy and energy dispersive microanalysis*, Microchimica Acta, 135, 121-130.

Zhao, J., **Li, W.**, **Luo, H.** & **Miao, J.,** 2010, *Research on protection of the architectural glazed ceramics in the Palace Museum, Beijing*, Journal of Cultural Heritage, 11, 279-287.

Zichler, R., **Ocskay, R.** & **Salma, I.,** 2007, *Story of air pollution of Budapest*, Air Working group, Eötvös Loránd University, Budapest. 103 p.

Received at: 24. 09. 2015
Revised at: 20. 03. 2016
Accepted for publication at: 04. 04.2016
Published online at: 13. 04. 2016